materials

MDPI

Article

Non-Isothermal Dynamic Mechanical Analysis of Ribbon Metallic Glasses and Its Thermodynamic Description

Arseniy Berezner * and Victor Fedorov

Theoretical and Experimental Physics Department, Derzhavin Tambov State University, Internatsionalnaya str. 33, 392000 Tambov, Russia

* Correspondence: a.berezner1009@gmail.com

Abstract: In this work, derivation of the main thermodynamic relationships is realized together with the applied calculation of some parameters, providing the systematized description of non-linear thermo-mechanical deformation at dynamic mechanical analysis (DMA). Obtained equations and values agree well with experiments on different ribbon metallic glasses. We generalize the main initial conditions (i.e., experimental and numerical parameters) by that the proposed model can be used for the investigation of DMA in different materials. The further opportunities of the found approach are also discussed in frames of phase transitions in metallic glass.

Keywords: metals and alloys; cyclic deformation; external energy influences

Citation: Berezner, A.; Fedorov, V. Non-Isothermal Dynamic Mechanical Analysis of Ribbon Metallic Glasses and Its Thermodynamic Description. *Materials* **2022**, *15*, 8659. https://doi.org/10.3390/ma15238659

Academic Editor: Sergey V. Konovalov

Received: 3 November 2022
Accepted: 1 December 2022
Published: 5 December 2022

1. Introduction

Formally, the study of deformation in materials has been developing in physics and technics since the forming of different scientific fields [1]. After comprehensive investigations of the elastic response in materials [2], scientists observed isothermal [3] or non-isothermal [4] creep and internal friction [5]. The investigated materials varied from metals [6] or simple inorganic compositions [7] to complex polymer systems [8]. Some deformation features (for example, yield drop, non-linear plastic stage and so on) appearing at elasto-plastic deformation also are described in frames of the different structural models [9]. Viscoelastic deformation is quite well described both in continuum mechanics [10] and by the semi-empirical models [11]. However, non-isothermal conditions (with different regimes of mechanical loading) are not properly investigated due to the absence of a general model describing the temporal or temperature deformation function. One of them is in material response to variable (uniform in time) heating with periodic force impact (dynamic mechanical analysis, i.e., DMA) [12]. The study of this deformation case by model generalization is of interest in physics and technics not only from fundamental but also from applied standpoints.

Along with corrosion [13] and magnetic [14] properties, mechanical parameters of different amorphous alloys (AMA) have been intensively investigated [15] since the first synthesis of metallic glass (MG) [16]. As these materials have some quantitative advantage by the mentioned properties, analysis of their behavior is more actual for the industry [17]. Viscosity [18] and dynamic properties [19] are intensively investigated in MG under different conditions (such as annealing [20] and rolling [21]), but mainly elastic (Kelvin–Voigt) deformation stage is the most investigated yet. Traditionally, an analogy is drawn between amorphous alloys, polymers and liquids [22] because the interatomic disordered structure is typical for these materials and substances [23]. However, the differences between their chemical composition and state must be accounted, and that is not always taking place because of insufficient data on this matter. For example, the Kauzmann paradox [24] is proposed to exist for metallic glasses [25] but not for all cases of their deformation, the analytical view of entropy function and other parameters, mentioned in the original work

(i.e., in [24]), is known. Thus, taking into account described points and other ones, thermodynamic description (with applied calculations) of cyclic inelastic deformation (DMA) of as-prepared and rolled MG is the main goal of this work.

2. Materials and Methods

As a basement for this investigation, our previous experimental data on DMA of Al- and Cu-based ribbon amorphous alloys (with ~40 μm of thickness and 4.5 mm of width) were chosen [26–28]. The general conditions for DMA are in the presence of F_{load}. Preloading (constant during an experiment) and oscillating (with $\omega = 6\pi$ rad/s frequency and A amplitude) force, which impact a specimen together. Moreover, continuous heating of alloy (with $V_T = 5$ K/min constant rate) from the heater was carried out in t time that led to break of the specimen in the B moment. During experiment, each specimen elongates from l_0~18.5 mm of working size (at potentially variable length) up to the critical maximum (~27 mm). Further model analysis must be carried out, starting from our previous equations, which were obtained in [26] for l variable deformation and $F_{react.}$ reaction force:

$$l(t) = l_0 + \frac{Ct}{B^2 - Bt}, \tag{1}$$

$$F_{react.}(\omega; t(T)) = F_{load} - A\sin(\omega t) - \frac{2mC}{(B-t)^3}. \tag{2}$$

For uniform temporal heating, from T_0 (~300 K) temperature to variable T one (not above ~550 K and 568 K crystallization temperatures of Al-based and Cu-based MG, consequently), we can write the time–temperature relationship:

$$t = \frac{T - T_0}{V_T} = \frac{\Delta T}{V_T}. \tag{3}$$

Moreover, T and T_0 are temperatures of the environment near the specimen (the pure temperature of alloy cannot be precisely measured because of technical calorimetric principles). In our experiments, different parasitic thermal effects (such as self-heating) arising at cyclic deformation in other systems [29] are not registered by a pyrometer or thermocouple. For Al- and Cu-based alloys, the mean values, presented in Table 1, are typical, among which C is a personal deformation coefficient, and m corresponds to the mass of a specimen.

Table 1. Experimental parameters and personal material values of investigated MG.

Alloy (at.%)	C, [m·s]	B, [s]	m, [kg]	F_{load}, [N]	A, [N]
$Al_{85}Y_8Ni_5Co_2$	0.078	3157	10^{-4}	3.6	0.0036
$Cu_{54}Pd_{28}P_{18}$	0.0492	2827	10^{-4}	0.9	0.0063

Generally, parameters in Equations (1)–(3) can take different numbers, depending on variable values of DMA. Further model derivations will be realized based on the described Equations (1)–(3) and data from Table 1.

3. Results and Discussion

Before solving a thermodynamic problem, the boundaries of investigated system with external and internal parameters [30] are necessary to determine. Thus, let us consider the «load-specimen» or «machine grip-specimen» system, characterized by $a = l$ (length) external parameter and T temperature, and that is heated with δQ amount (of heat) for change its dU internal energy with further doing of δW work on its environment (i.e., work of a specimen on the machine grip and force sensors). With respect to the construction features of the DMA machine, its furnace can be considered a container that does not exchange heat with external space. As a generalized force in this system, reaction one

(2) is chosen, and its analytical form can be represented as a function both of length and temperature [28]:

$$F_{react.}(l;T) = F_{load} - A\sin\left(\omega\frac{T-T_0}{V_T}\right) - \frac{2mC}{\left(B-\frac{B^2(l-l_0)}{C+B(l-l_0)}\right)^2\left(B-\frac{T-T_0}{V_T}\right)}. \quad (4)$$

Moreover, preloading force (i.e., F_{load}) is already accounted for the description of the initial system state, and, therefore, the elastic (post-preloading) transition process in a specimen is not necessary for consideration at DMA. Such delimitation in the system permits optimal modeling of the oscillating force as an inner process instead as a part of the external work performed on the specimen. This feature is also justified by the anharmonic amplitude-frequency response of the specimen (due to the change of the $\omega(T)$ in the sinus argument of Equation (2) or (4)) in some range at further temperature growth [26,28]. Thus, the volume of the thermodynamic system is set some larger than the personal sizes of a specimen, but all its parts preserve or change reversibly their properties, unlike alloy, which deforms.

For a more valid model derivation and further analysis of DMA, the mentioned Equation (4) also can be checked with thermodynamic criteria of a state function. It is possible to do this with generalized force (4) by the equation of a differential form [31]. In this case, equality of the mixed partial derivatives $\left(\frac{\partial^2 F_{react.}(l;T)}{\partial l\partial T}\right)_T = \left(\frac{\partial^2 F_{react.}(l;T)}{\partial T\partial l}\right)_l$ takes place, and both parts are equal to $-\frac{4mB^2C^2}{V_T\left(B-\frac{T-T_0}{V_T}\right)^5(C+B(l-l_0))^2}$. On the whole $\Sigma(l;T)$ definition domain and trajectory $l(T)$, i.e., on a deformation curve (process), the function (4) is continuous. Therefore, proposed equations can be considered for a deterministic description of deformation because $F_{react.}$ value is the state function, described by an equation of state, i.e., by Equation (4), on the $\Sigma(l;T)$ connected domain. Note that, because of the metastable initial state, the deformation of metallic glass can be considered in frames of equilibrium thermodynamics with a possible change of the obtained equations onto inequalities at non-equilibrium conditions (for example, near the crystallization temperature). As the thermal equation of state is known, the caloric one, i.e., full internal energy, can be found. From the first thermodynamic law $\delta Q = dU + \delta W$, full energy ΔU will be determined as the difference between whole heat ΔQ and work ΔW. Moreover, this law (equation) is integrated with respect to the deformation process (L($l(T)$;T) with a non-linear trajectory), taking into account Equation (4), i.e., as $\int\limits_L \delta Q = \int\limits_L dU + \int\limits_L \delta W = \int\limits_L dU + \int\limits_L F_{react.}(l;T)dl$. We also notice that curvilinear integral over δQ must be conditionally equalized to the full amount of heat received from an electric heater in a furnace (by Joule's law)

$$\Delta Q = Pt = P\frac{\Delta T}{V_T} \quad (5)$$

where P is electrical heater power and t is heating duration according to Equation (3). This condition can give some overvalue number for real heating of alloy because of secondary heat transfer from the thermal element to inner furnace walls and environment of a specimen. However, this value has a fixed limit, not exceeding all generated heat (5), and it permits estimation of the system dynamics up to the constant difference. Actually, the amount of heat, passing only through the specimen, could be calculated with the different thermal models (such as Fourier or Maxwell–Cattaneo laws) instead of Equation (5), but the real heat flow dynamic and its spatial distribution in the alloy are hard to estimation from

the experimental standpoint. Therefore, we use standard full estimation (5) for analysis. After curvilinear integration of δW, an equation for work at DMA of MG has a form:

$$\Delta W = \frac{F_{load}C(T-T_0) - AC\Theta(T-T_0)}{BV_T\left(B-\frac{T-T_0}{V_T}\right)} + \frac{C^2m\left(\left(B-\frac{T-T_0}{V_T}\right)^4 - B^4\right)}{2B^4\left(B-\frac{T-T_0}{V_T}\right)^4}, \quad (6)$$

where Θ ($|\Theta| \leq 1$) is a multiplier of $\int_{T_0}^{T} \frac{AC\sin\left(\frac{\omega(T-T_0)}{V_T}\right)}{V_T\left(B-\frac{T-T_0}{V_T}\right)^2}dT$, according to the mean value theorem [31], which takes place at curvilinear integration, then, full internal energy will be determined as:

$$\Delta U = \Delta Q - \Delta W = P\frac{\Delta T}{V_T} - \frac{(F_{load}C - AC\Theta)(T-T_0)}{BV_T\left(B-\frac{T-T_0}{V_T}\right)} - \frac{C^2m\left(\left(B-\frac{T-T_0}{V_T}\right)^4 - B^4\right)}{2B^4\left(B-\frac{T-T_0}{V_T}\right)^4}. \quad (7)$$

Analysis of Equation (6) shows that work conducted in the considered system is positive that corresponds to the action of the deformation force, directed along a total shift of the machine grip. Up to the term of supplied heat, the full internal energy of the specimen decreases during deformation (see Figure 1).

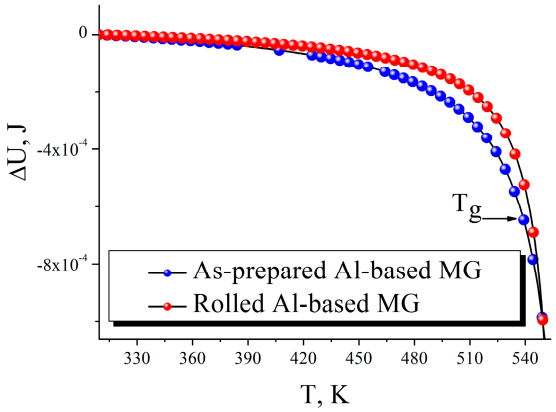

Figure 1. Change of full internal energy in $Al_{85}Y_8Ni_5Co_2$ MG with rolling (red dots) or without it (blue dots). The glass-transition temperature (T_g) is mentioned with the arrow.

The calculated curves in Figure 1 correlate with our hypothesis (in the collective work [28]) about structural rearrangement to a more uniform change of full internal energy after rolling. It also agrees with our interpretation that rolled and as-prepared specimens achieve joint minimal energy points near T_g (~540 K) [28]. Amplitude-frequency and phase-frequency modulations, arising at the deformation of amorphous alloys [26–28], do not sufficiently impact the main decrease tendency of function (7), but some variation for its rate takes place. Change of C and B parameters corresponds quantitatively with the thermodynamic functions (4)–(7) that also testifies about the strong relationship between these values and the deformation conditions of the material. Moreover, by Equation (7), we obtain the same tendency for Cu-based alloy (decrease of $\Delta U(T)$ up to the minimum), and it changes faster near personal B time (2827 s) than for Al-based one. The difference in energy dynamics of both alloys (if we compare their B parameters from Table 1) causes a relatively earlier fracture of the Cu-based ribbon. However, any comparison of these alloys in an amorphous state is limited by T_g of copper-based MG (528 K) [27].

In some works on metallic glass thematic (such as described in the review [32]), the structural condition is described in frames of energy Arrhenius model, i.e., by Maxwell–Boltzmann (generally, Gauss) statistics. Moreover, this approach is often supposed to

be applicable for the glass transition region. However, by definition [33], the mentioned statistics take place in the equilibrium state with a predominantly fixed temperature that obstructs the model using in more complex cases (for example, in a non-isothermal process with loading or at a phase transform point). Someone can note the necessity in a more complex modified exponential function at a strong behavioral deviation of alloy from ideal normal distribution [34]. These features make necessary a thermodynamic estimation of statistics in the conditions of DMA.

By opening the brackets in Equation (7) with further term division of the numerator by the denominator, full internal energy can be represented in a form:

$$\Delta U = P\frac{\Delta T}{V_T} - \frac{F_{load}C}{B - \frac{T-T_0}{V_T}} + \frac{F_{load}C}{B} + \frac{AC\Theta}{B - \frac{T-T_0}{V_T}} - \frac{AC\Theta}{B} + \frac{C^2m}{2\left(B - \frac{T-T_0}{V_T}\right)^4} - \frac{C^2m}{2B^4}. \quad (8)$$

Then, the remembered expression of $\langle U(T)\rangle$ mean (i.e., expected) energy by its distribution (and probability density function, i.e., PDF) [33], we can write the equations:

$$\Delta U(T_{1/2}) \sim \langle U(T)\rangle = \int_T U(T)f(T)dT; \quad (9a)$$

$$\frac{d\langle U(T)\rangle}{dT} = U(T)f(T) \sim \frac{d(\Delta U(T_{1/2}))}{dT} = \\ = \frac{P}{V_T} - \frac{F_{load}C}{V_T\left(B - \frac{T_{1/2}-T_0}{V_T}\right)^2} + \frac{AC\Theta}{V_T\left(B - \frac{T_{1/2}-T_0}{V_T}\right)^2} + \frac{2C^2m}{V_T\left(B - \frac{T_{1/2}-T_0}{V_T}\right)^5}, \quad (9b)$$

where $T_{1/2}$ is the mean experimental temperature (~430 K), $\Delta U(T_{1/2})$ is the function value of (8) at the middle-temperature point, $f(T)$ is a derivative of the distribution function (in the differential $dP(T) = P'(T)dT = f(T)dT$, i.e., PDF. $T_{1/2}$ can be considered as a variable if we describe the whole experimental data array, i.e., variation of the experimental mean point is taken into account for different DMA tests occurring for the same alloy system (specimen set) in frames of Equation (8). In the second term of (9b), we note the $U_1 = \frac{F_{load}C}{B - \frac{T_{1/2}-T_0}{V_T}}$ multiplier, also being in (8), and write the recurrent equation (that takes place not only in $T_{1/2}$ point but at different T):

$$\frac{dU_1}{dT} = \frac{U_1}{V_T\left(B - \frac{T-T_0}{V_T}\right)}, \quad (10)$$

which is a differential one with separated variables, and its general solution (i.e., U_1) can be represented in a form:

$$U_1 = M_1 \exp\left(\int \frac{dT}{V_T\left(B - \frac{T-T_0}{V_T}\right)}\right) \quad (11a)$$

where M_1 is an integration constant. Performing similar steps in the third and fourth terms in (9b), let us derive equations:

$$U_2 = M_2 \exp\left(\int \frac{dT}{V_T\left(B - \frac{T-T_0}{V_T}\right)}\right), \; U_3 = M_3 \exp\left(\int \frac{4dT}{V_T\left(B - \frac{T-T_0}{V_T}\right)}\right) \quad (11b)$$

in which M_2 and M_3 are integration constants of the corresponding differential equations. By substitution of (11a) and (11b) in the left part of (9a) instead U_1, U_2 and U_3 with M_0 notation for a sum of all remained terms, we find the relationship:

$$M_0 + M_1 \exp(\tau) + M_2 \exp(\tau) + M_3 \exp(4\tau) \sim \langle U(T) \rangle = \int_T U(T) f(T) dT, \quad (12)$$

where $\tau = \int \frac{dT}{V_T\left(B - \frac{T-T_0}{V_T}\right)}$. Using the mean value theorem for the integral in (12), let us derive the expression:

$$M_0 + M_1 \exp(\tau) + M_2 \exp(\tau) + M_3 \exp(4\tau) \sim \langle U(T) \rangle = \overline{u} \int_T f(T) dT \quad (13)$$

where both parts can be divided by $\overline{u}$ (i.e., mean value of $U(T)$ at $T \sim T_{1/2}$), and after differentiation by T, the final estimation form for PDF will be found as:

$$\alpha_0 + \alpha_1 \exp(\tau) + \alpha_2 \exp(\tau) + \alpha_3 \exp(4\tau) \sim f(T) \quad (14)$$

with α_k exponential coefficients (i.e., the quotients of $M_k/\overline{u}$, (k = 0–3)).

As seen from (14), $f(T)$ can be described by the sum of exponents, and its normalizing condition $\int_T f(T) dT = 1$ will be determined by the equality between $\overline{u}$ and the sum in the left part of (13), i.e., the precise equation between $\langle U(T) \rangle$ and $\Delta U(T_{1/2})$ is potentially possible at $T = T_{1/2}$ (or description will be qualitative at $T \sim T_{1/2}$). Moreover, the number of terms (depending on M_k) and value of τ argument in exponents provide the view of $f(T)$ in each experiment. This variation of the coefficients can lead to quite different functional representations, which have a similar curve form but not the same interpolation accuracy for the experiment. Integrals in exponent arguments (i.e., in Equation (11a,b)) also can be considered in frames of mean value theorem that gives $\sim \exp\left(\frac{\Delta T}{V_T(B - \Delta T_{1/2} V_T^{-1})}\right)$ an expression for them. Moreover, by exact integration in τ, $\sim \frac{1}{B - \Delta T_{1/2} V_T^{-1}}$ expression is an alternative form for the same equations with analogous functional behavior, compared with exponents. The existence of many analytical representations for $f(T)$ (also at the numerical fitting of experiments [32]) can be caused by a change of interaction behavior between atoms and molecules in metallic glass. Arrhenius equation is typical for more ideal equilibrium systems with independent «particles» interacting elastically with one another [33]. The presence of non-elastic pair interactions between «particles» leads to a change of PDF and related values, which can be observed in Debye's and Einstein's works on heat capacity or in Van der Waals's article, for example [35]. During DMA of amorphous alloys with heating above room temperatures, probable anharmonic interaction of the atoms and molecules is similar to simultaneous periodical stretching of many elastic and non-elastic springs, acting between material points. In this case, the collective resonance effects with specific experimental signals (relaxation maxima, beating and so on) are possible.

In frames of applied thermodynamics, molar capacity and thermal expansion coefficient are often determined. Moreover, the estimation of entropy change in a process is an important task. As we derive the main functions of the state, an analysis of the described parameters can be provided. Particularly, from Equation (5), the average entropy change function has a form:

$$\Delta S = \frac{\Delta Q}{T} = P \frac{\Delta T}{T V_T}, \quad (15)$$

and its plot is depicted in Figure 2.

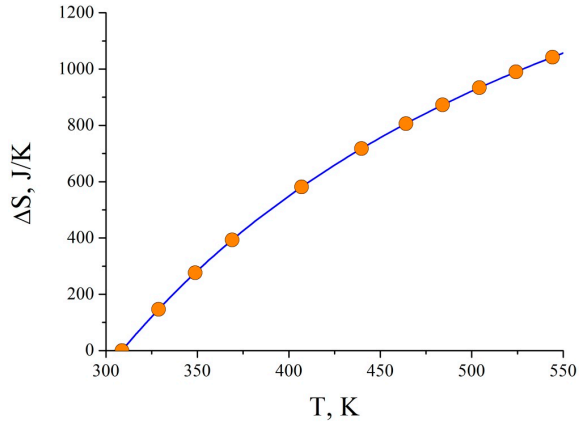

Figure 2. Entropy change at DMA of Al-based and Cu-based amorphous alloys.

As seen from Figure 2, non-isothermal deformation with mechanical loading is in equilibrium only at room temperature (initial conditions) because $\Delta S = 0$. The further temperature growth leads to the development of a non-equilibrium process ($\Delta S > 0$). Therefore, using only equilibrium models (such as Maxwell–Boltzmann statistics) appears to be ineffective in the high-temperature range. Moreover, from Equation (15), we can notice that temperature impact is the main source of the entropy change, i.e., thermal activation is a distinctive feature for this type of experiment.

Previously [36], we calculated linear thermal expansion coefficient (CLTE), whose number value agreed with the experiment up to the integer part of a number and magnitude order (α_L~$4{\cdot}10^{-6}$–$6{\cdot}10^{-6}$ 1/K for Cu-based and Al-based MG, consequently). It permits estimation of molar heat capacity, which relates with CLTE linearly by γ Gruneisen parameter [37] for many materials. In most cases, precise analytical derivation of γ is complicated by different factors, but this proportion coefficient can be specified empirically. As known [38], the thermal capacity of amorphous alloys varies less intensively, unlike partially crystallized (i.e., post-annealed) one, near T_g. However, the estimation of this value by «crystalline» data gives a confidential interval. From the literature [39], we observe that the ratio between molar heat capacity C_{mol} and CLTE (i.e., $b = C_{mol}/\alpha_L$) changes on 15–30 units for most crystalline alloys, and, therefore, C_{mol} for Al- and Cu-based metallic glasses lies between the numbers $\alpha_L \cdot b$ = 60–180 J/(mol·K). This result agrees with experimental data by the magnitude order both for crystalline and amorphous alloys [40,41]. Some our model relationships can be considered as a basement for analysis of the different systems or conditions, such as complex deformation of Al-based [42] or Ti-based alloys [43].

4. Conclusions

In this work, we carried out consistent calculations of the main thermodynamic relations for Al- and Cu-based amorphous alloys, which underwent acting of uniform (in time) heating and oscillating mechanical load. Non-equilibrium deformation behavior, which limits using of Maxwell–Boltzmann statistics in a wide high-temperature interval (above room ones), has been shown. CLTE and molar heat capacity, which are sensitive to molecular rearrangements, are calculated in frames of the proposed model. Moreover, our model corresponds quite precisely with experimental data from the different works on amorphous and crystalline thematics. Derived relationships can be used to analyze DMA in different materials that demonstrate the same behavior in similar conditions. Using the thermal and caloric state equations permits analysis of cyclic processes and system stability (by potentials) that can give additional information about different properties of the investigated systems near phase transition points.

Author Contributions: Conceptualization, A.B. and V.F.; methodology, A.B.; validation, A.B. and V.F.; formal analysis, A.B.; data curation, A.B.; writing—original draft preparation, A.B.; writing—review and editing, V.F.; supervision, V.F.; project administration, V.F. All authors have read and agreed to the published version of the manuscript.

Funding: This work was supported by the Russian Science Foundation (grant No. 22-22-00226). The results were partially obtained using the equipment of the Center for Collective Use of Scientific Equipment of Derzhavin Tambov State University. This work was partially supported by the Ministry of Science and Higher Education of the Russian Federation in the framework of agreement No. 075-15-2021-709 (unique project identifier RF—2296.61321X0037).

Institutional Review Board Statement: Not applicable.

Informed Consent Statement: Not applicable.

Data Availability Statement: Not applicable.

Conflicts of Interest: The authors declare no conflict of interest.

References

1. Meyers, M.; Chawla, K. *Mechanical Behavior of Materials*, 2nd ed.; Cambridge University Press: Cambridge, UK, 2008; pp. 1–882.
2. Rees, D.W.A. *Basic Engineering Plasticity*; Butterworth-Heinemann: Oxford, UK, 2006; pp. 1–528.
3. Da Costa Andrade, E.N. On the viscous flow in metals, and allied phenomena. *Proc. R. Soc. Lond. A* **1910**, *84*, 1–12.
4. Khonik, V.A.; Mikhailov, V.A.; Safonov, I.A. Non-isothermal creep of metallic glasses. *Scr. Mater.* **1997**, *37*, 921–928. [CrossRef]
5. De Batist, R. *Internal Friction of Structural Defects in Crystalline Solids*; North-Holland Publishing Company: Amsterdam, The Netherlands, 1973; pp. 1–477.
6. Liu, C.; Liu, P.; Zhao, Z.; Northwood, D.O. Room temperature creep of a high strength steel. *Mater. Des.* **2001**, *22*, 325–328. [CrossRef]
7. Cannon, W.R.; Langdon, T.G. Creep of ceramics. *J. Mater. Sci.* **1988**, *18*, 1–20. [CrossRef]
8. Raghavan, J.; Meshii, M. Creep of polymer composites. *Compos. Sci. Technol.* **1998**, *57*, 1673–1688. [CrossRef]
9. Lomer, W.M. The yield phenomenon in polycrystalline mild steel. *J. Mech. Phys. Solids* **1952**, *1*, 64–73. [CrossRef]
10. Wagner, M.H. Analysis of time-dependent non-linear stress-growth data for shear and elongational flow of a low-density branched polyethylene melt. *Rheol. Acta* **1976**, *15*, 136–142. [CrossRef]
11. Wilkinson, W. *Non-Newtonian Fluids*; Pergamon Press: Oxford, UK, 1960; pp. 1–138.
12. Menard, K.P. *Dynamic Mechanical Analysis: A practical Introduction*; CRC Press: Boca Raton, FL, USA, 1999; pp. 1–205.
13. Pluzhnikova, T.N.; Fedorov, V.A.; Balybin, D.V.; Berezner, A.D.; Mikhlin, Y.L.; Fedotov, D.Y. Solid-Phase Hydrogen Diffusion through a $Fe_{92}Si_6B_6$ Amorphous Membrane and its Effect on the Mechanical Properties of a Non-Crystalline Environment. *Prot. Met. Phys. Chem. Surf.* **2021**, *57*, 1235–1241. [CrossRef]
14. Berezner, A.D.; Fedorov, V.A.; Perov, N.S.; Pluzhnikova, T.N.; Fedotov, D.Y.; Shlikova, A.A. Magnetic properties of Co-based and Fe-based tape amorphous alloys. *J. Phys. Condens. Matter* **2020**, *32*, 1–9. [CrossRef]
15. Louzguine-Luzgin, D.V.; Zadorozhnyy, M.Y.; Ketov, S.V.; Jiang, J.; Golovin, I.S.; Aronin, A.S. Influence of cyclic loading on the structure and double-stage structure relaxation behavior of a Zr-Cu-Fe-Al metallic glass. *Mater. Sci. Eng. A* **2019**, *742*, 526–531. [CrossRef]
16. Duwez, P. Structure and Properties of Alloys Rapidly Quenched from the Liquid State. *Trans. Am. Soc. Metals.* **1967**, *60*, 607–633.
17. Lenel, F.V.; Ansell, G.S. Creep Mechanisms and Their Role in the Sintering of Metal Powders. In *Modern Developments in Powder Metallurgy*; Hausner, H.H., Ed.; Springer: Berlin/Heidelberg, Germany, 1966; pp. 281–296.
18. Ketov, S.V.; Inoue, A.; Kato, H.; Louzguine-Luzgin, D.V. Viscous flow of $Cu_{55}Zr_{30}Ti_{10}Co_5$ bulk metallic glass in glass-transition and semi-solid regions. *Scr. Mater.* **2013**, *68*, 219–222. [CrossRef]
19. Zadorozhnyy, V.Y.; Zadorozhnyy, M.Y.; Churyumov, A.Y.; Ketov, S.V.; Golovin, I.S.; Louzguine-Luzgin, D.V. Room-temperature dynamic quasi-elastic mechanical behavior of a Zr–Cu–Fe–Al bulk metallic glass. *Phys. Status Solidi A* **2016**, *213*, 450–456. [CrossRef]
20. Bazlov, A.I.; Igrevskaya, A.G.; Tabachkova, N.Y.; Chen, C.; Cheverikin, V.V.; Pozdniakov, A.V.; Jiang, J.; Louzguine-Luzgin, D.V. Thermo-mechanical processing of a $Zr_{62.5}Cu_{22.5}Fe_5Al_{10}$ glassy alloy as a way to obtain tensile ductility. *J. Alloy. Compd.* **2021**, *853*, 1–10. [CrossRef]
21. Louzguine-Luzgin, D.V.; Inoue, A. Comparative study of the effect of cold rolling on the structure of Al–RE–Ni–Co (RE = rare-earth metals) amorphous and glassy alloys. *J. Non-Cryst. Solids* **2006**, *352*, 3903–3909. [CrossRef]
22. Inoue, A.; Wang, X.M.; Zhang, W. Developments and applications of bulk metallic glasses. *Rev. Adv. Mater. Sci.* **2008**, *18*, 1–9.
23. Anderson, P.W. Through the Glass Lightly. *Science* **1995**, *267*, 1615–1616. [CrossRef]
24. Kauzmann, W. The Nature of the Glassy State and the Behavior of Liquids at Low Temperatures. *Chem. Rev.* **1948**, *43*, 219–256. [CrossRef]

25. Mitrofanov, Y.P.; Khonik, V.A.; Granato, A.V.; Joncich, D.M.; Khonik, S.V.; Khoviv, A.M. On the nature of enthalpy relaxation below and above the glass transition of metallic glasses. *Appl. Phys. Lett.* **2012**, *100*, 131903. [CrossRef]
26. Berezner, A.D.; Fedorov, V.A.; Zadorozhnyy, M.Y.; Golovin, I.S.; Louzguine-Luzgin, D.V. Deformation of $Al_{85}Y_8Ni_5Co_2$ Metallic Glasses under Cyclic Mechanical Load and Uniform Heating. *Metals* **2021**, *11*, 908. [CrossRef]
27. Berezner, A.D.; Fedorov, V.A.; Zadorozhnyy, M.Y.; Golovin, I.S.; Louzguine-Luzgin, D.V. Deformation of Cu-Pd-P metallic glass under cyclic mechanical load on continous heating. *Theor. Appl. Fract. Mech.* **2022**, *118*, 103262. [CrossRef]
28. Berezner, A.D.; Fedorov, V.A.; Zadorozhnyy, M.Y. Relaxation behavior of an Al-Y-Ni-Co metallic glass in as-prepared and cold-rolled state. *J. Alloy. Compd.* **2022**, *923*, 166313. [CrossRef]
29. Wang, G.Y.; Liaw, P.; Peter, W.H.; Yang, B.X.; Freels, M.; Yokoyama, Y.; Benson, M.L.; Green, B.A.; Saleh, T.A.; Mcdaniels, R.; et al. Fatigue behavior and fracture morphology of $Zr_{50}Al_{10}Cu_{40}$ and $Zr_{50}Al_{10}Cu_{30}Ni_{10}$ bulk-metallic glasses. *Intermetallics* **2004**, *12*, 1219. [CrossRef]
30. Whitman, A.M. *Thermodynamics: Basic Principles and Engineering Applications*; Springer: Berlin/Heidelberg, Germany, 2019; pp. 1–320.
31. Zorich, V.A. *Mathematical Analysis I (Universitext)*, 2nd ed.; Springer: Berlin/Heidelberg, Germany, 2015; pp. 1–616.
32. Wang, W.H. Dynamic relaxations and relaxation-property relationships in metallic glasses. *Prog. Mater. Sci.* **2019**, *106*, 100561. [CrossRef]
33. McQuarrie, A. *Statistical Mechanics*; Harper & Row: New York, NY, USA, 1976; pp. 1–641.
34. Dyre, J.C. Colloquium: The glass transition and elastic models of glass-forming liquids. *Rev. Mod. Phys.* **2006**, *78*, 953. [CrossRef]
35. Van der Waals, J.D. *Over de Continuiteit van den Gasen Vloeistoftoestand*; Sijthoff: Leiden, The Netherlands, 1873.
36. Berezner, A.; Fedorov, V.; Grigoriev, G. A few fracture features of Al-based and Cu-based ribbon metallic glasses under non-isothermal and oscillating loading. *Lect. Notes Mech. Eng.* **2023**, 1–8.
37. Podgornykh, S.M.; Kazantsev, V.A. Relationship between the heat capacity, thermal expansion coefficient, and spontaneous magnetization in the invarlike compound YFe10Mo2. *Phys. Met. Metallogr.* **2010**, *109*, 247–254. [CrossRef]
38. González, S.; Pellicer, E.; Suriñach, S.; Baró, M.D.; Sort, J. Mechanical and corrosion behaviour of as-cast and annealed $Zr_{60}Cu_{20}Al_{10}Fe_5Ti_5$ bulk metallic glass. *Intermetallics* **2012**, *28*, 149–155. [CrossRef]
39. Barsoum, M.W.; Rawn, C.J.; Ei-Raghy, T.; Procopio, A.; Porter, W.D.; Wang, H.; Hubbard, C. Thermal properties of Ti_4AlN_3. *J. Appl. Phys.* **2000**, *87*, 8407. [CrossRef]
40. Calvin, J.J.; Asplund, M.; Zhang, Y.; Huang, B.; Woodfield, B.F. Heat capacity and thermodynamic functions of γ-Al_2O_3. *J. Chem. Thermodyn.* **2017**, *112*, 77–85. [CrossRef]
41. Suryanarayana, C.; Inoue, A. *Bulk Metallic Glasses*, 2nd ed.; CRC Press: Boca Raton, FL, USA, 2020; pp. 1–542.
42. Gromov, V.E.; Ivanov, Y.F.; Stolboushkina, O.A.; Konovalov, S.V. Dislocation substructure evolution on Al creep under the action of the weak electric potential. *Mater. Sci. Eng. A* **2010**, *527*, 858–861. [CrossRef]
43. Konovalov, S.V.; Komissarova, I.A.; Kosinov, D.A.; Ivanov, Y.F.; Ivanova, O.V.; Gromov, V.E. The structure of the titanium alloy, modified by electron beams and destroyed during fatigue. *Lett. Mater.* **2017**, *7*, 266–271. [CrossRef]